

Generation of a physiologically relevant *in vitro* model of autosomal dominant Retinitis Pigmentosa caused by *RHO-P23H* mutation using 3D retinal organoids

Chichagova V¹, Atkin W¹, Tomlinson BK¹, Malaczkowski D¹, Puri D¹, Kay M¹, Georgiou M¹, Ramsay K¹, Brittain N¹, Devlin C¹, Novelli R², Aramini A³, Amendola P⁴, Sirico A⁴, Gándara C¹
¹Newcells Biotech Limited, Newcastle upon Tyne, UK; ²Dompé farmaceutici, Milan, Italy; ³Dompé farmaceutici, L'Aquila, Italy; ⁴Dompé farmaceutici, Naples, Italy

5302

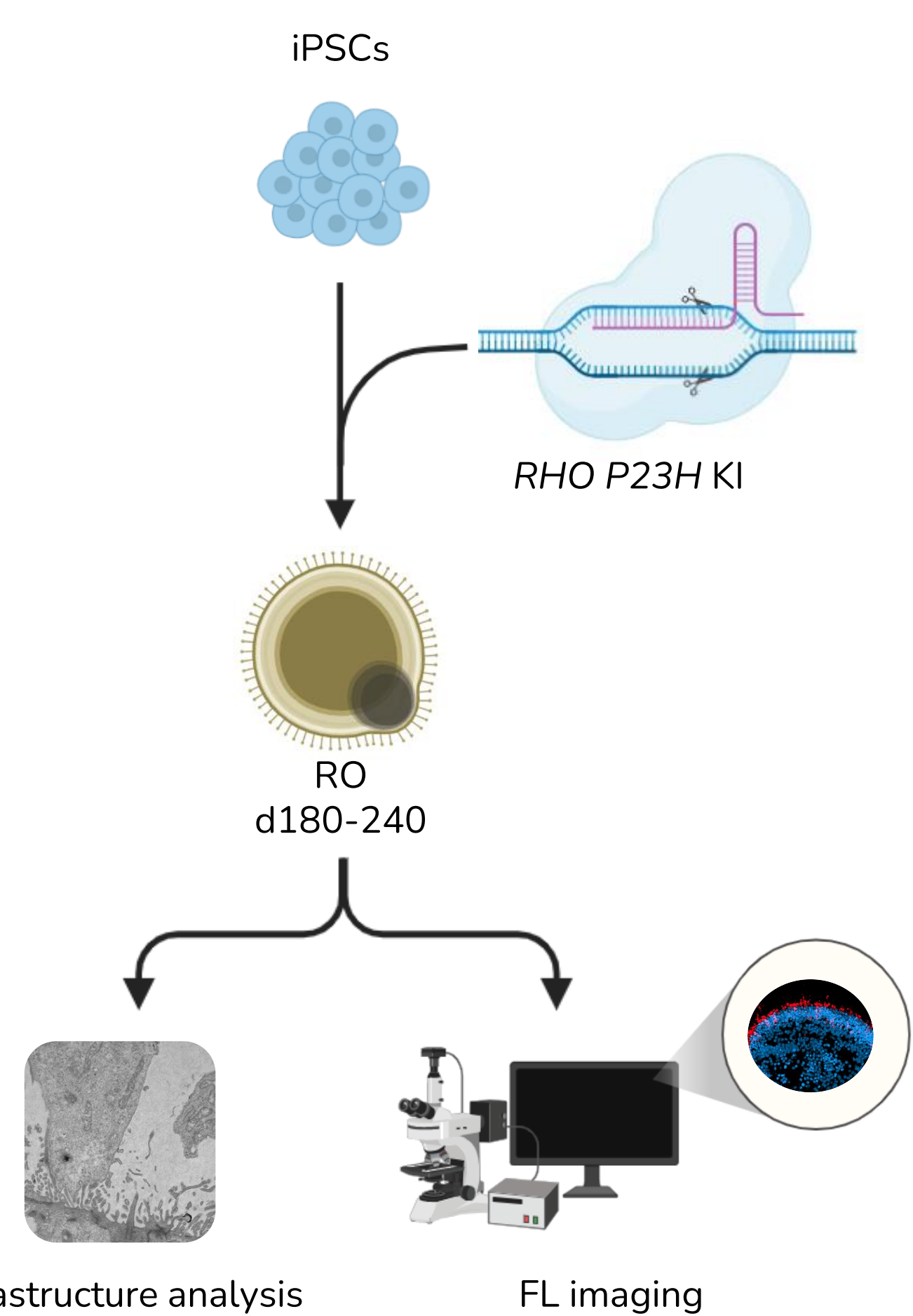
Purpose

Retinitis Pigmentosa (RP) is a group of inherited retinal degenerative diseases that affects 1 in 4,000 people worldwide. Mutations in the *RHO* gene are the main cause of autosomal dominant RP (adRP), which accounts for ~20-30% of total RP cases. *RHO-P23H* is the most common variant out of more than 100 mutations in the *RHO* gene associated with adRP. Animal models for adRP, particularly those expressing the P23H Rhodopsin variant, show discrepancies depending on the type of model generated. Therefore, the aim of this study was to generate a human physiologically relevant adRP-*RHO-P23H* *in vitro* model to better understand the disease mechanisms and ultimately improve clinical translation of new therapies to patients with adRP.

Methods

A heterozygous P23H knock-in mutation was introduced into the *RHO* gene of human iPSCs derived from a healthy donor using CRISPR-Cas9-mediated gene editing. *RHO-P23H* and the isogenic control iPSC lines were differentiated to retinal organoids (ROs) and cultured until maturation at 180-240 days. Comparisons between the mutant (*RHO-P23H*) and control (NCB WT) organoids were performed by characterising their morphology, protein expression profile, and cellular ultrastructure (Figure 1).

Figure 1. Experimental summary.



Results

I. Photoreceptors

- Protein expression of the rod marker, RHO, significantly increased in *RHO-P23H* organoids at d180 compared to NCB WT. Differences were not significant at d210 or d240 (Figures 2&3).
- Protein expression of the cone marker, OPN1MW/LW, significantly increased in *RHO-P23H* organoids at all timepoints compared to NCB WT (Figures 2&4).

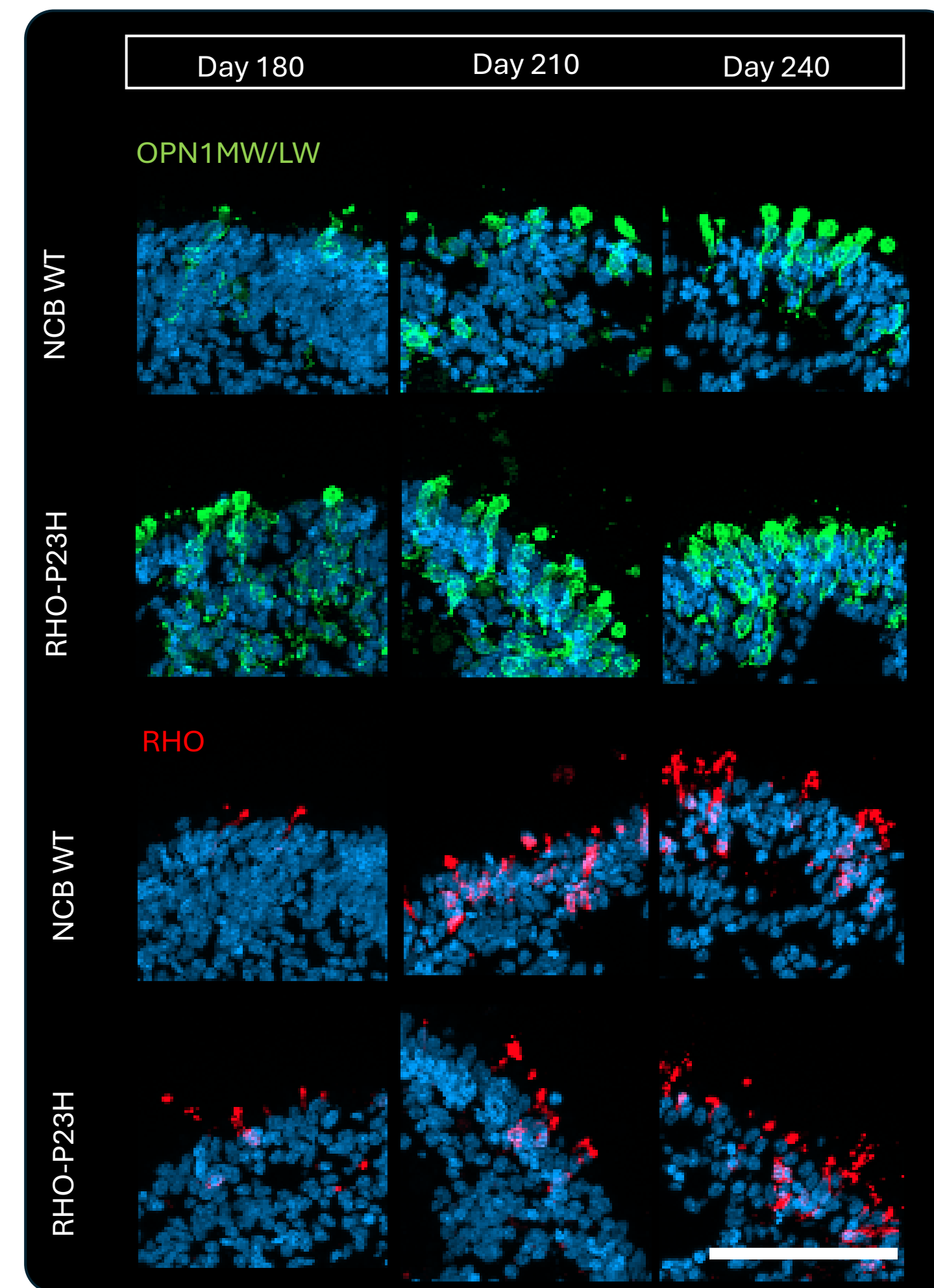


Figure 2. Representative immunofluorescence images of RO at day 180, 210 and 240 of differentiation. Scale bar = 50 μm.

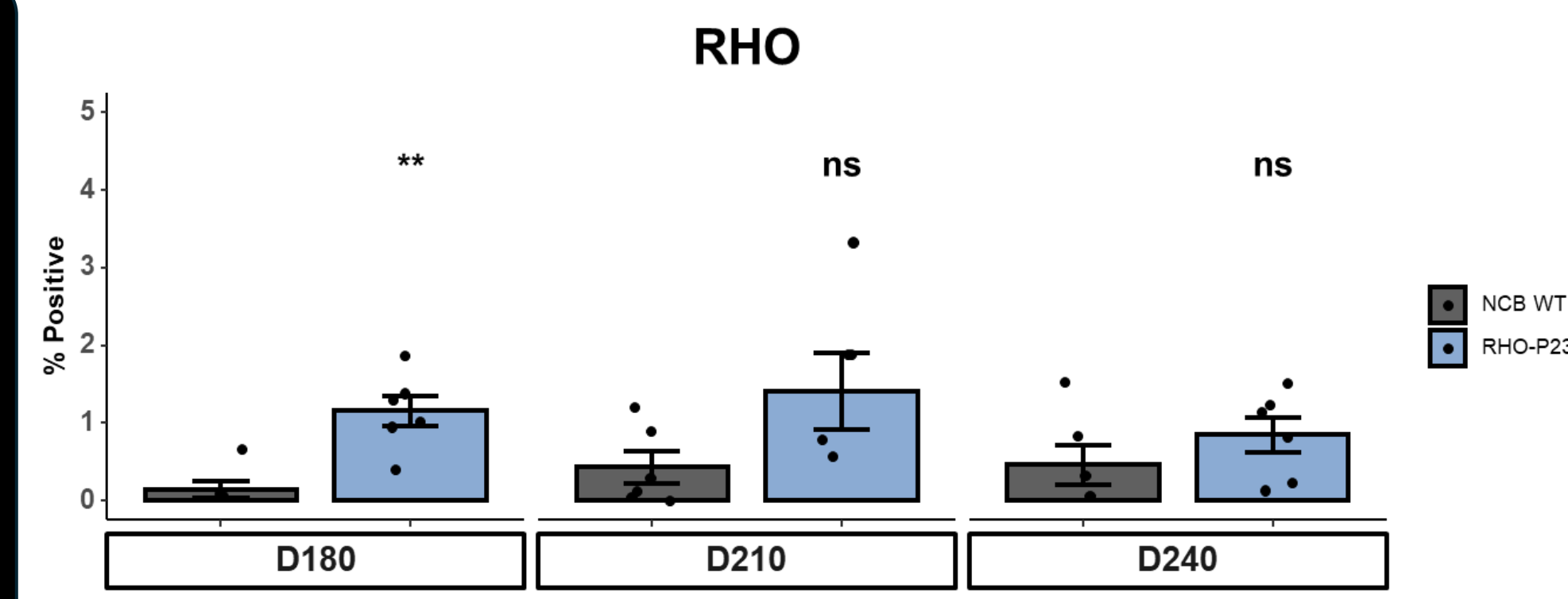


Figure 3. IF quantification of rod photoreceptors. ROs were stained, quantified for percentage positivity and analysed for differences between *RHO-P23H* and NCB WT ROs within each timepoint by t-test. n=6 ROs per condition. Data bars represent mean ± SD, individual points represent quantification of single ROs.

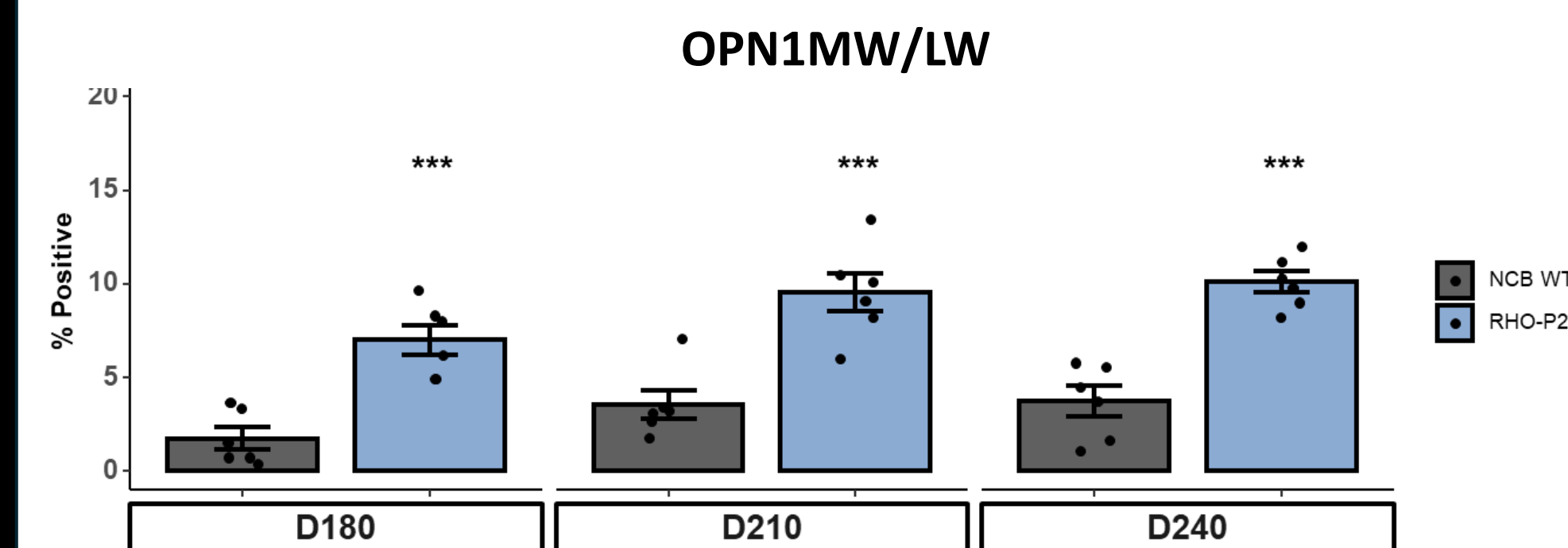


Figure 4. IF quantification of cone photoreceptors. ROs were stained, quantified for percentage positivity and analysed for differences between *RHO-P23H* and NCB WT ROs within each timepoint by t-test. n=6 ROs per condition. Data bars represent mean ± SD, individual points represent quantification of single ROs.

II. Connecting cilia

- Expression of the cilia marker, ARL13B, was significantly lower in *RHO-P23H* ROs compared to NCB WT at d180 and d210 (Figure 5).
- ARL13B expression was also lower at d240 although not statistically significant (Figure 6).

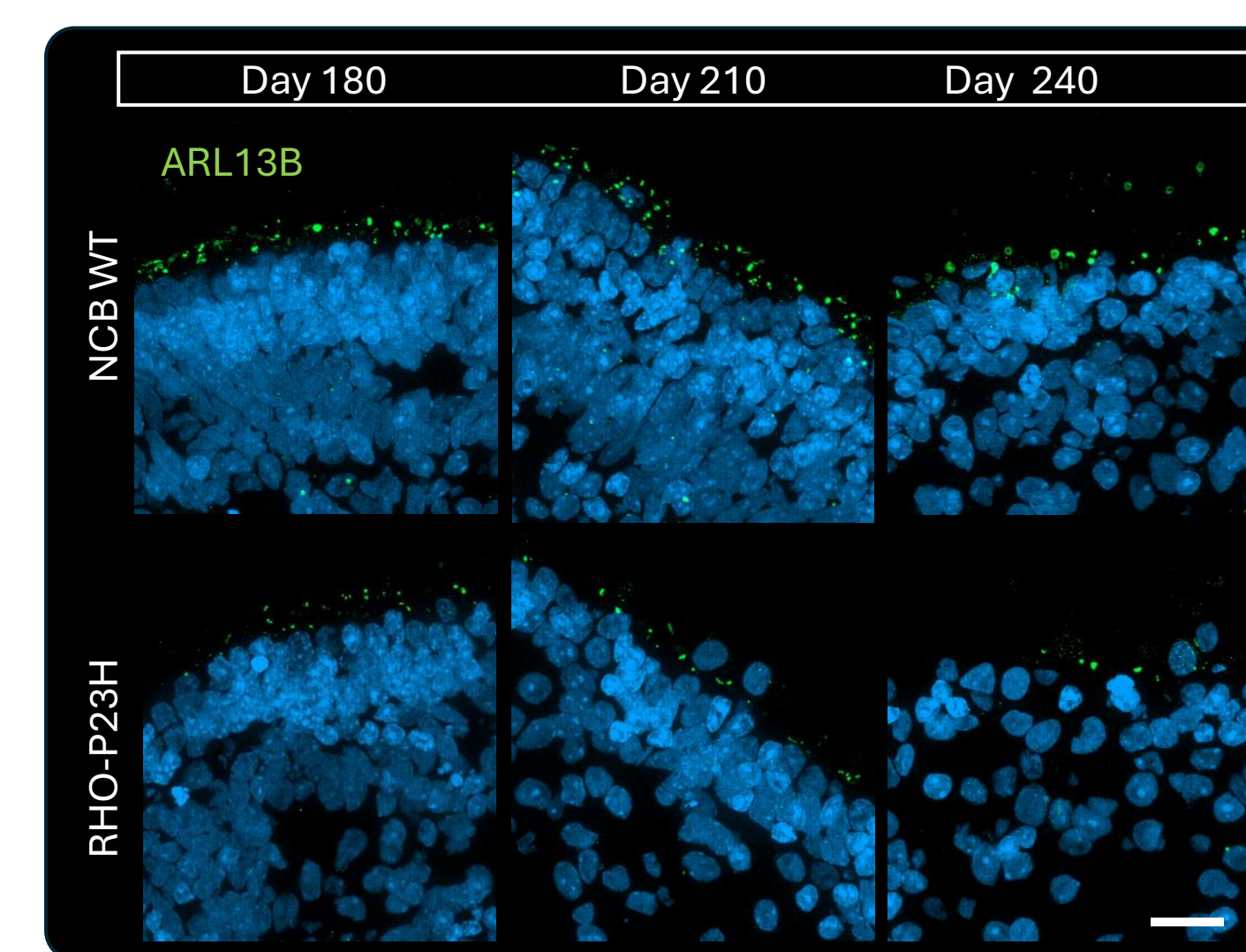


Figure 5. Immunofluorescence RO images at d180, d210 and d240 of differentiation from NCB-WT and *RHO-P23H* iPSC lines. Scale bar = 20 μm.

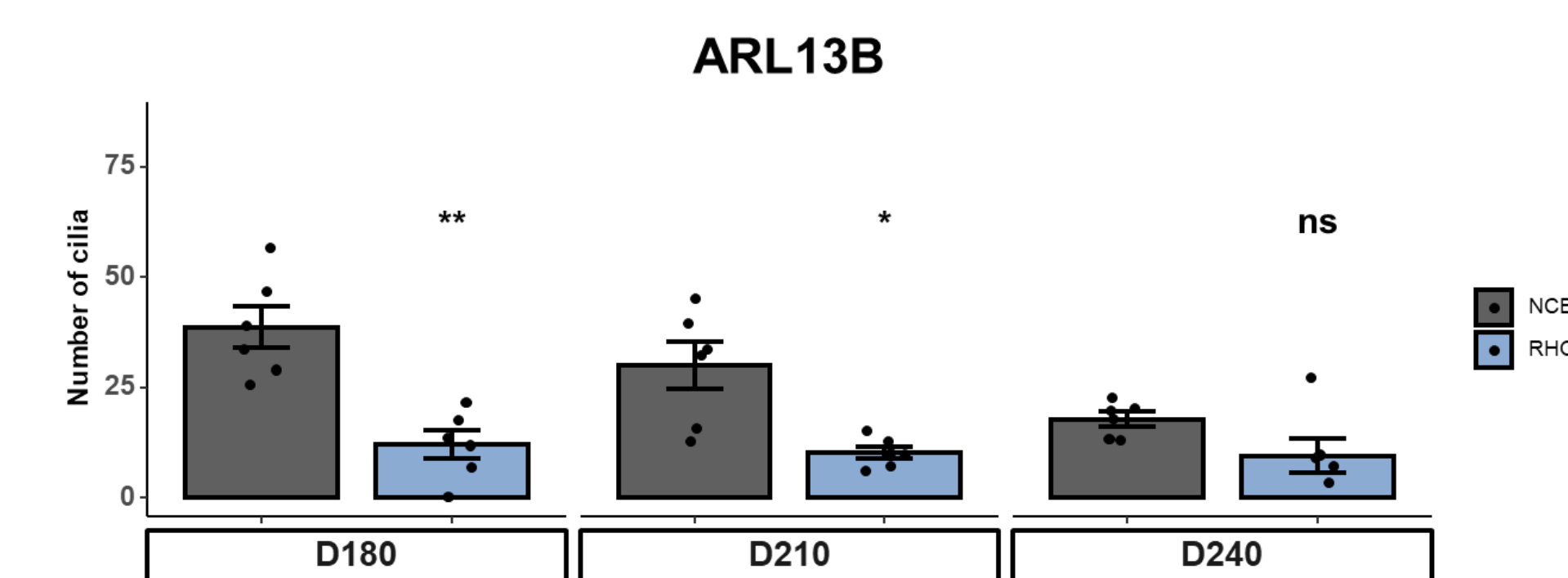


Figure 6. A: ROs were stained, quantified for number of cilia and analysed for differences between *RHO-P23H* and NCB WT ROs within each timepoint by t-test. n=6 ROs per condition. Data bars represent mean ± SD, individual points represent quantification of single ROs.

III. Astrocytes

- *RHO-P23H* ROs had significantly lower area of expression of the astrocyte marker GFAP, at d180 and d240 compared to NCB WT. There was a similar trend at d210 (Figures 7&8).

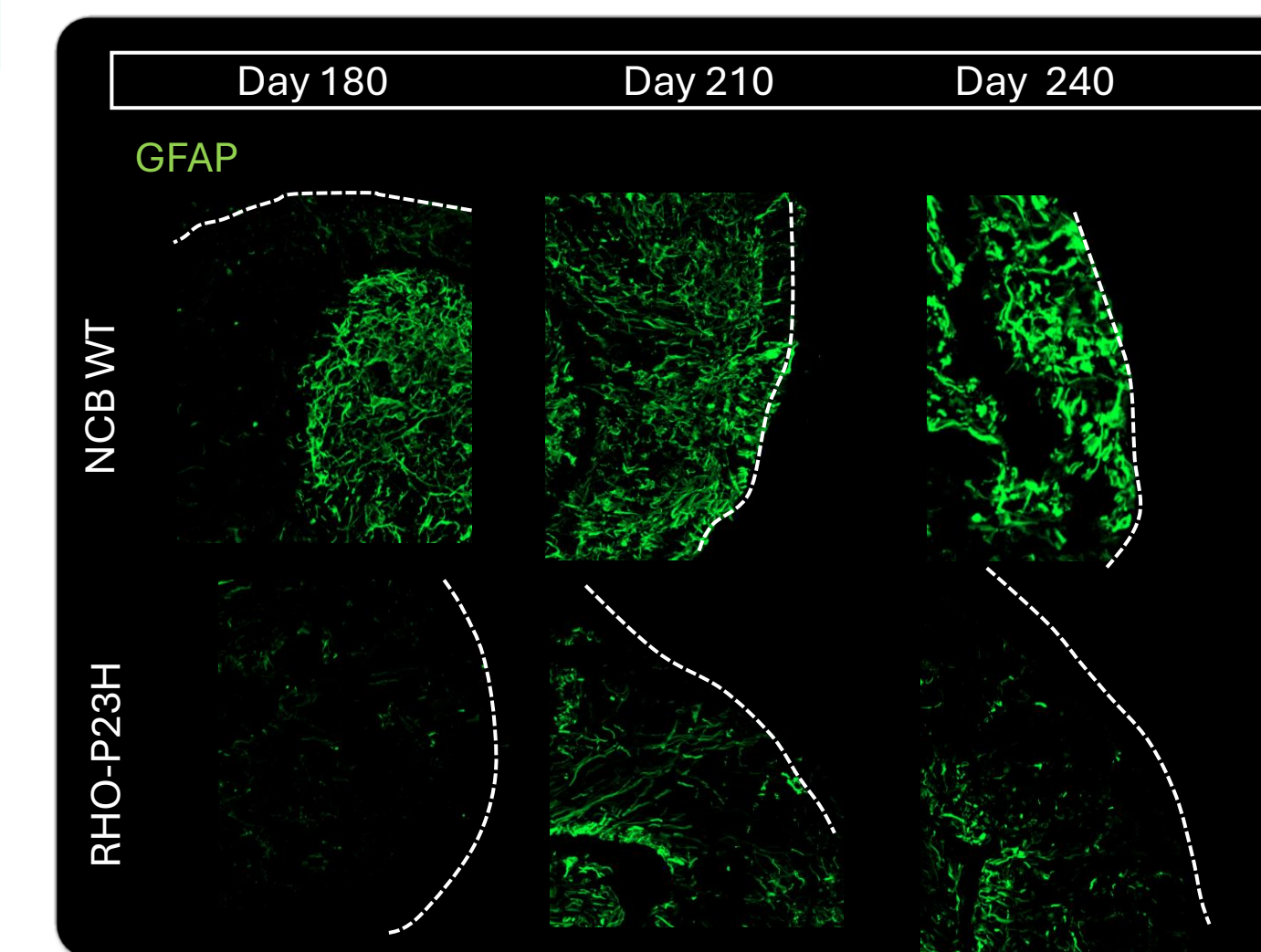


Figure 7. Representative immunofluorescence images of RO at day 180, 210 and 240 of differentiation. Scale bar = 100 μm.

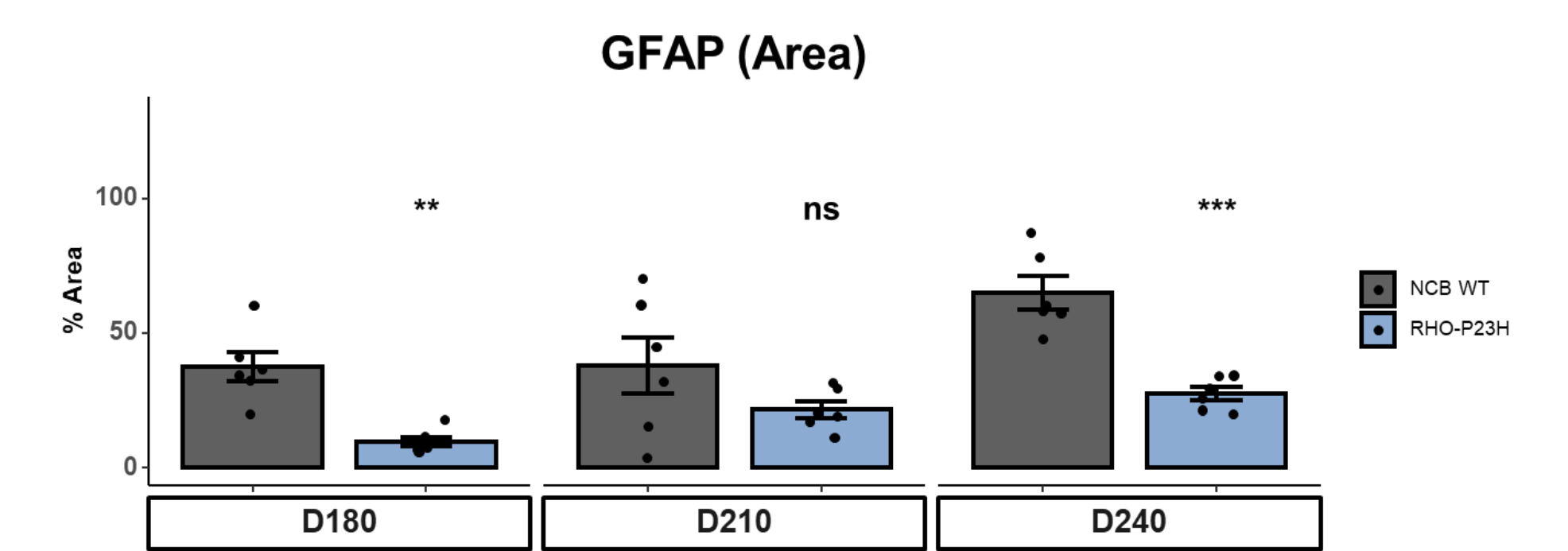


Figure 8. IF quantification of astrocytes. ROs were stained, quantified for percentage positive area, and analysed for differences between *RHO-P23H* and NCB WT ROs within each timepoint by t-test. n=6 ROs per condition. Data bars represent mean ± SD, individual points represent quantification of single ROs.

IV. Transmission Electron Microscopy (TEM)

- *RHO-P23H* ROs showed increased signs of cellular stress with a higher presence of stress vacuoles compared to NCB WT (Figures 9).

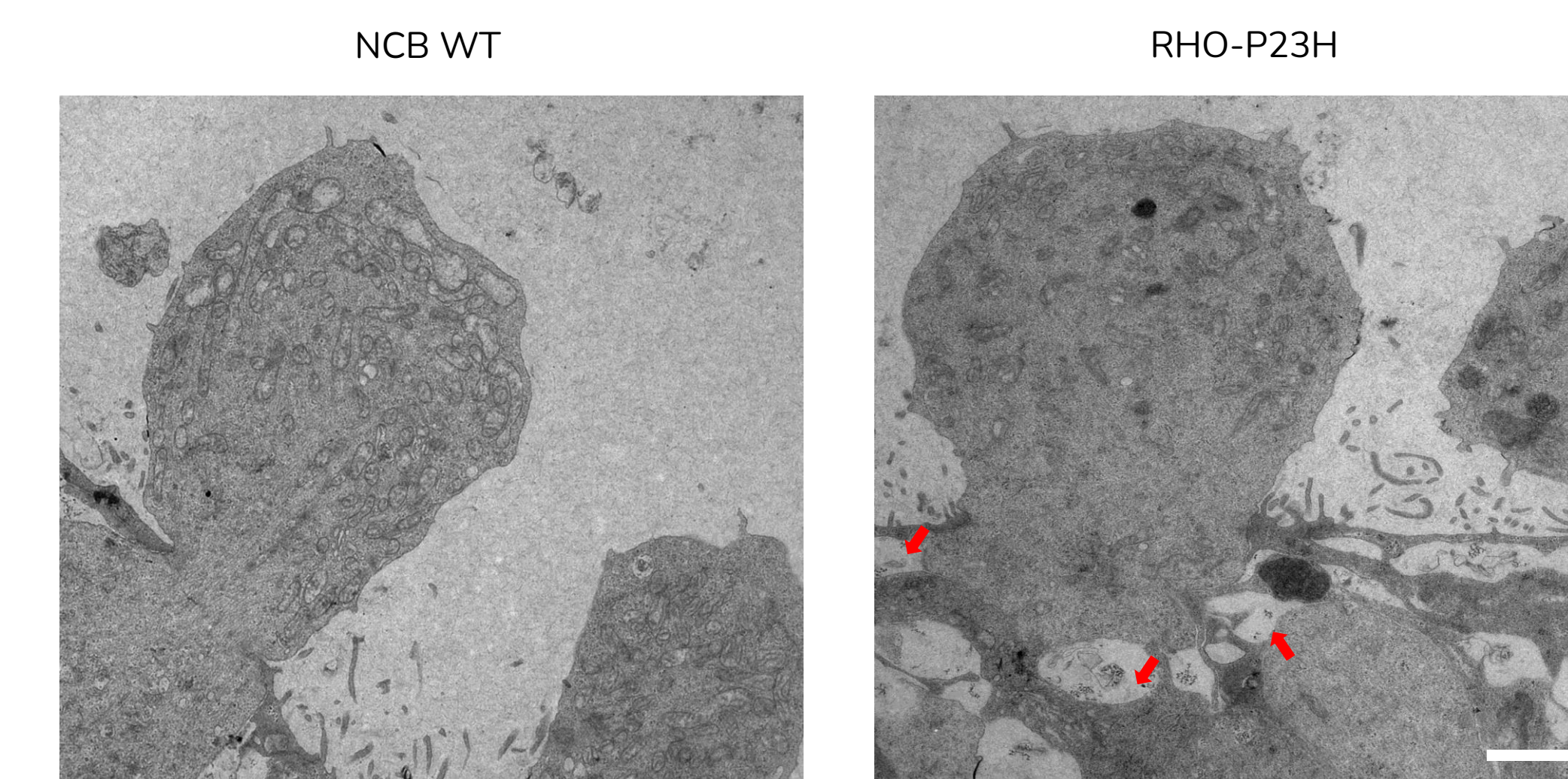


Figure 9. TEM Images of NCB-WT and *RHO-P23H* retinal organoids at day 210. Red arrows indicate the presence of stress vacuoles. Scale bar = 2 μm.

Conclusions

This study establishes a human physiologically relevant *in vitro* model of adRP-*RHO-P23H*. Compared to controls, mutant retinal organoids showed higher expression of mature rod and cone photoreceptor proteins across multiple timepoints. *RHO-P23H* disease organoids also exhibited a significant reduction in ARL13B+ cilia, especially at day 180, and decreased GFAP expression area at later time points. Additionally, mutant organoids showed increased signs of stress such as higher presence of stress vacuoles. Reduction in cilia numbers in the absence of reduced photoreceptor proteins could be indicative of increased translation but defective trafficking into the outer segments. Astrocytes play a complex role in retinal disease pathogenesis and may impact retinal neuronal survival and retinal function. Overall, this model offers valuable insight into the pathophysiology of adRP and provides a promising platform to support early drug development and guide preclinical decision-making.



Further details available online or contact us at info@newcellsbiotech.co.uk



NEWCELLS
IN VITRO MODELS TO ACCELERATE CLINICAL TRANSLATION